

# Universal low-temperature properties of frustrated classical spin chain near the ferromagnet-helimagnet transition point

D. V. Dmitriev\* and V. Ya. Krivnov

*Joint Institute of Chemical Physics, RAS, Kosygin str. 4, 119334, Moscow, Russia.*

(Dated:)

The thermodynamics of the classical frustrated spin chain near the transition point between the ferromagnetic and the helical phases is studied. The calculation of the partition and spin correlation functions at low temperature limit is reduced to the quantum mechanical problem of a particle in potential well. It is shown that the thermodynamic quantities are universal functions of the temperature normalized by the chiral domain wall energy. The obtained behavior of the static structure factor indicates that the short-range helical-type correlations existing at low temperatures on the helical side of the transition point disappear at some critical temperature, defining the Lifshitz point. It is also shown that the low-temperature susceptibility in the helical phase near the transition point has a maximum at some temperature. Such behavior is in agreement with that observed in several materials described by the quantum  $s = 1/2$  version of this model.

## I. INTRODUCTION

Strongly frustrated low-dimensional magnets attracted much attention last years [1]. A very interesting class of such compounds is edge-sharing chains where  $CuO_4$  plaquets are coupled by their edges [2–5]. An important feature of the edge-sharing chains is that the nearest-neighbor (NN) interaction  $J_1$  between  $Cu$  spins is ferromagnetic while the next-nearest-neighbor (NNN) interaction  $J_2$  is antiferromagnetic. The competition between them leads to the frustration. A minimal model describing the magnetic properties of these cuprates is so-called F-AF spin chain model the Hamiltonian of which is

$$H = J_1 \sum \mathbf{S}_n \cdot \mathbf{S}_{n+1} + J_2 \sum \mathbf{S}_n \cdot \mathbf{S}_{n+2} \quad (1)$$

where  $J_1 < 0$  and  $J_2 > 0$ .

The ground state phase diagram of the  $s = 1/2$  F-AF model has been studied extensively last years [6–12]. The ground state of this model is governed by the frustration parameter  $\alpha = J_2/|J_1|$ . At  $0 < \alpha < 1/4$  the ground state is fully ferromagnetic. At  $\alpha > 1/4$  the incommensurate singlet phase with short-range helical spin correlations is realized. At  $\alpha = 1/4$  the quantum phase transition occurs. Remarkably, this transition point does not depend on a spin value, including the classical limit  $s \rightarrow \infty$ .

However, the influence of the frustration on low temperature thermodynamics is less studied, especially in the vicinity of the ferromagnet-helimagnet transition point. It is of a particular importance to study this problem, because there are several edge-sharing cuprates with  $\alpha \simeq 1/4$  which are of special interest [13].

Unfortunately, at present the low-temperature thermodynamics of quantum  $s = 1/2$  model (1) at  $\alpha \neq 0$  can be studied only either by using of numerical calculations of finite chains or by approximate methods. On the other hand, the classical version of model (1) can be studied exactly at  $T \rightarrow 0$ . It is expected that the main qualitative features of the quantum low-temperature thermodynamics can be reproduced correctly in the framework of the classical model. Besides, the classical limit can be used as a starting point to study quantum effects. Therefore, the study of classical model (1) is useful for the understanding of the low-temperature properties of the quantum F-AF chains.

At zero temperature classical model (1) has magnetic long range-order (LRO) for all values of  $\alpha$ : the ferromagnetic LRO at  $\alpha \leq 1/4$  and the helical-type LRO with the wave number  $Q = \cos^{-1}(1/4\alpha)$  for  $\alpha > 1/4$ . It should be noticed that both the time-reversal and the parity symmetries are broken in the helical ordered phase. The helical ordered state possesses a two-fold discrete chiral degeneracy (in addition to the usual spin-rotational degeneracy) corresponding to clockwise and counter-clockwise turn of spins. The chiral order parameter is defined by the chirality vector  $\vec{K}_n = [\vec{S}_n \times \vec{S}_{n+1}]$ . At finite temperature the LRO is destroyed by thermal fluctuations, the thermodynamic quantities have singular behavior at  $T \rightarrow 0$  with the corresponding critical exponents depending on  $\alpha$ . In Ref.[14] we studied classical model (1) at  $\alpha = 1/4$ , i.e. exactly at the ferromagnet-helimagnet transition point. It was shown that

---

\*Electronic address: dmitriev@deom.chph.ras.ru

the correlation length  $l_c$  behaves as  $T^{-1/3}$  and zero-field susceptibility  $\chi$  diverges as  $T^{-4/3}$  in contrast with the 1D Heisenberg ferromagnet (HF) ( $\alpha = 0$ ) where  $l_c \sim T^{-1}$  and  $\chi \sim T^{-2}$  [15].

In this paper we focus on the low-temperature thermodynamics of the F-AF classical model in the vicinity of the ferromagnet-helimagnet transition point. As it will be shown, in the low-temperature limit the thermodynamic quantities become the universal functions of the scaled temperature  $t = T/\gamma^{3/2}$ , where the parameter  $\gamma = (4\alpha - 1)$  characterizes the deviation from the transition point and is assumed to be small. The calculation of the thermodynamic quantities in this limit reduces to the solution of the Schrödinger equation for the quantum particle in an anharmonic potential.

It is worth noting that the thermodynamics of classical spin model (1) has been studied before [16, 17] using the transfer-matrix method with the subsequent solution of the corresponding integral equations by Gaussian integration formulas. This method gives reliable results for the moderate temperatures and values of  $\gamma$ . However, this procedure fails for low temperatures because of appearing of an artificial gap in the excitation spectrum [18]. Our approach gives exact asymptotics of the thermodynamic quantities at  $T \rightarrow 0$ ,  $\gamma \rightarrow 0$  and these results are complementary to those obtained in [16, 17].

The paper is organized as follows. In Section II the continuum version of the model is introduced. The problem of the calculation of the partition function is reduced to the solution of the Schrödinger equation for a particle in the potential well. In Section III the spin correlation function is obtained and the  $k$ -dependence of the static structure factor is studied. It is shown that the low temperature thermodynamics is the universal function of the scaling variable. The phase diagram of the model is constructed and the location of the Lifshitz point is determined. The behavior of the chiral correlation function is also studied. In Section IV the summary of the obtained results is given and their relation to early studies of the considered model [16, 17] is discussed. In the Appendix the derivation of the energy of chiral domain wall is given.

## II. PARTITION FUNCTION

In the vicinity of the transition point it is convenient to rewrite Hamiltonian (1) in the form [19]:

$$H = \frac{1}{8} \sum [(\mathbf{S}_{n+1} - 2\mathbf{S}_n + \mathbf{S}_{n-1})^2 - \gamma(\mathbf{S}_{n+1} - \mathbf{S}_{n-1})^2] \quad (2)$$

where  $\gamma = (4\alpha - 1)$ .

In Eq.(2) we put  $|J_1| = 1$  and omit unessential constant. In the classical approximation the spin operators  $\mathbf{S}_n$  are replaced by the classical unit vectors  $\vec{S}_n$ . We will investigate mainly the case  $\gamma > 0$  corresponding to the helical side of the ground state phase diagram. In the limit  $T \rightarrow 0$  the thermal fluctuations are weak and at  $\gamma \rightarrow 0$  the period of the helix is long, so that neighbor spins are directed almost parallel to each other. Therefore, we can use the continuum approach replacing  $\vec{S}_n$  by the classical unit vector field  $\vec{s}(x)$  with slowly varying orientations, so that

$$\vec{S}_{n+1} - \vec{S}_{n-1} \approx 2 \frac{\partial \vec{s}(x_n)}{\partial x} \quad (3)$$

and

$$\vec{S}_{n+1} - 2\vec{S}_n + \vec{S}_{n-1} \approx \frac{\partial^2 \vec{s}(x_n)}{\partial x^2} \quad (4)$$

where the lattice constant is chosen as unit length.

Using Eqs.(3) and (4) Hamiltonian (2) goes over into the energy functional of the vector field  $\vec{s}(x)$ :

$$E = \frac{1}{8} \int dx \left[ \left( \frac{\partial^2 \vec{s}}{\partial x^2} \right)^2 - 4\gamma \left( \frac{\partial \vec{s}}{\partial x} \right)^2 \right] \quad (5)$$

This energy functional is a starting point of the investigations of model (1) in the vicinity of the transition point  $\alpha = 1/4$ . The partition function is a functional integral over all configurations of the vector field on a ring of length  $L$

$$Z = \int D\vec{s}(x) \exp \left\{ -\frac{1}{8T} \int_0^L dx \left[ \left( \frac{\partial^2 \vec{s}}{\partial x^2} \right)^2 - 4\gamma \left( \frac{\partial \vec{s}}{\partial x} \right)^2 \right] \right\} \quad (6)$$

It is useful to scale the spatial variable as

$$\xi = 2T^{1/3}x \quad (7)$$

Then, the partition function takes the dimensionless form

$$Z = \int D\vec{s}(\xi) \exp \left\{ - \int_0^\lambda d\xi \left[ \left( \frac{d^2\vec{s}}{d\xi^2} \right)^2 - b \left( \frac{d\vec{s}}{d\xi} \right)^2 \right] \right\} \quad (8)$$

where

$$b = \frac{\gamma}{T^{2/3}} \quad (9)$$

and the rescaled system length is  $\lambda = 2T^{1/3}L$ .

Since the integration in the partition function occurs over all possible spin configurations, we are free to choose any local coordinate system. It is convenient to choose it so that the  $z$  axis at the point  $\xi$  is directed along the spin vector  $\vec{s}(\xi)$ , so that the spin vector  $\vec{s}(\xi) = (0, 0, 1)$ .

Let us introduce a new vector field

$$\vec{q}(\xi) = \frac{d\vec{s}}{d\xi} = (q_x, q_y, q_z) \quad (10)$$

Then, the constraint  $\vec{s}^2(\xi) = 1$  converts to the relations for  $\vec{q}(\xi)$ :

$$\begin{aligned} q_z &= 0 \\ q'_z &= -q_x^2 - q_y^2 \end{aligned} \quad (11)$$

where the prime denotes the space derivative  $d/d\xi$ .

Then, the first term of the Hamilton function in Eq.(5) transforms to

$$\left( \frac{d^2\vec{s}}{d\xi^2} \right)^2 = \left( \frac{d\vec{q}}{d\xi} \right)^2 = q_x'^2 + q_y'^2 + (q_x^2 + q_y^2)^2 \quad (12)$$

Here we see that the constraint  $\vec{s}^2 = 1$  effectively eliminates the  $q_z$  component from the Hamilton function. Therefore, henceforth we deal with the  $q_x$  and  $q_y$  components of the vector field  $\vec{q}$  only, and we denote a two-component vector field by  $\mathbf{q}(\xi) = (q_x, q_y)$ .

The partition function in terms of  $\mathbf{q}(\xi)$  takes the form:

$$Z = \int D\mathbf{q}(\xi) \exp \left\{ - \int_0^\lambda d\xi (\mathbf{q}'^2 + \mathbf{q}^4 - b\mathbf{q}^2) \right\} \quad (13)$$

If we replace  $\xi$  by an imaginary time  $\xi \rightarrow it$  then partition function (13) takes the form of a path integral of a quantum particle in a potential  $U(\mathbf{q}) = \mathbf{q}^4 - b\mathbf{q}^2$ . In other words  $Z$  in Eq.(13) is the partition function of the quantum system at ‘temperature’  $1/\lambda$  described by the Hamiltonian

$$\hat{H}_0 = -\frac{1}{4}\Delta + \mathbf{q}^4 - b\mathbf{q}^2 \quad (14)$$

where  $\Delta = \partial_x^2 + \partial_y^2$  is two-dimensional Laplace operator. Hamiltonian (14) commutes with the  $z$ -component of the angular momentum  $\hat{l}_z$  and eigenstates  $\psi(\mathbf{q})$  of the corresponding Schrödinger equation are divided into subspaces of azimuthal quantum numbers  $l_z = 0, \pm 1, \pm 2 \dots$

$$\hat{H}_0 \psi_{n,l_z} = \varepsilon_{n,l_z} \psi_{n,l_z} \quad (15)$$

Thus, the wave function  $\psi_{n,l_z}(\mathbf{q})$  describes a particle with the azimuthal quantum number  $l_z$  in the 2D axially symmetrical potential well  $U(q) = q^4 - bq^2$  ( $q = |\mathbf{q}|$ ). Obviously, the eigenfunctions and the eigenvalues of Eq.(15) are real for all values of  $b$ . The dependencies of several lowest eigenvalues of Eq.(15) on model parameter  $b$  are shown in Fig.1. For large  $b$  the potential  $U(q)$  takes the form of the Mexican hat with a deep and steep axially symmetrical well  $U(q) \approx 2b(q - \sqrt{b/2})^2 - b^2/4$ . In this case the spectrum becomes almost degenerate over angular momentum  $l_z$ , which is in accord with Fig.1. In the limit  $b \rightarrow \infty$  the asymptotic of eigenvalues of Eq.(15) can be found explicitly:

$$\varepsilon_{n,l_z} = -\frac{b^2}{4} + n\sqrt{2b} + \frac{l_z^2}{4b} \quad (16)$$

The partition function is a sum of exponents over all states and in the thermodynamic limit ( $\lambda = 2T^{1/3}L \rightarrow \infty$ ) only the lowest eigenvalue  $\varepsilon_0$  with  $n = l_z = 0$  gives contribution to the partition function:

$$Z = \sum_{n,l_z} e^{-\lambda \varepsilon_{n,l_z}} \rightarrow e^{-\lambda \varepsilon_0} \quad (17)$$

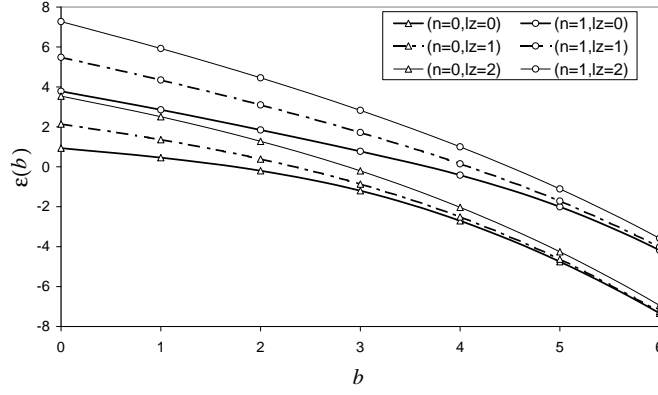


FIG. 1: Dependencies of several lowest eigenvalues  $\varepsilon_{n,l_z}$  (with  $n = 0, 1$  and  $l_z = 0, 1, 2$ ) of Eq.(15) on parameter  $b$ .

### III. CORRELATION FUNCTION

The calculation of the correlation function  $\langle \vec{s}(l) \cdot \vec{s}(0) \rangle$  is more complicated procedure in comparison with that for the partition function. It is considered in detail for the case  $\alpha = 1/4$  ( $b = 0$ ) in Ref.[14], where the problem of the calculation of the correlation functions reduces to solution of the additional differential equations together with Eq.(15). This procedure can be extended to the case  $\alpha \neq 1/4$  straightforwardly. In particular, the expressions for the correlation function remains exactly the same as for the case  $\alpha = 1/4$  and only the form of the potential well in the corresponding pair of differential equations is modified,  $U(\mathbf{q}) = \mathbf{q}^4 - b\mathbf{q}^2$  instead of  $U(\mathbf{q}) = \mathbf{q}^4$ . The differential equations are

$$\begin{aligned} -\frac{1}{4} \frac{d^2 v}{dq^2} - \frac{1}{4q} \frac{dv}{dq} + \frac{1}{4q^2} v + q^4 v - bq^2 v + qu &= \eta v \\ -\frac{1}{4} \frac{d^2 u}{dq^2} - \frac{1}{4q} \frac{du}{dq} + q^4 u - bq^2 u - qv &= \eta u \end{aligned} \quad (18)$$

Eqs.(18) represent the eigenvalue problem for  $\eta_n$  and eigenfunctions  $u_n(q)$  and  $v_n(q)$  satisfying the normalization conditions:

$$\langle u_n^* | u_m \rangle - \langle v_n^* | v_m \rangle = \delta_{n,m} \quad (19)$$

System of equations (18) describes a two-level system in the axially symmetric potential well  $U(\mathbf{q}) = \mathbf{q}^4 - b\mathbf{q}^2$ , where two levels with angular momenta  $l_z = 0$  and  $l_z = 1$  are coupled by non-Hermitian transition operator.

As shown in Ref.[14] the spin correlation function has a form

$$\langle \vec{s}(l) \cdot \vec{s}(0) \rangle = \sum_n \langle \psi_0 | u_n \rangle^2 e^{-2T^{1/3}(\eta_n - \varepsilon_0)l} \quad (20)$$

where  $\psi_0$  and  $\varepsilon_0$  are the ground state wave function and the ground state energy of the Schrödinger equation (15) and  $u_n$  and  $\eta_n$  are the eigenfunctions and the eigenvalues of Eqs.(18).

The numerical solution of Eqs.(18) demonstrates the following properties. For small  $b$  all eigenvalues of Eq.(18) are real but the eigenfunctions of Eq.(18) are complex. With the increase of  $b$ , two lowest levels  $\eta_{1,2}$  approach to each other, then at  $b_0 \simeq 0.145$  they coincide and after that, for  $b > b_0$ , these eigenvalues become complex conjugated. Their imaginary part increases as  $\Im(\eta_{1,2}) \sim \sqrt{(b - b_0)}/2$ . These features of the solutions of Eqs.(18) are illustrated in Fig.2, where the dependencies of the eigenvalues  $\eta_{1,2}$  on parameter  $b$  are shown. According to Eq.(20) the appearance of imaginary parts of eigenvalues  $\eta_n$  implies that the correlation function begins to oscillate.

With the further increase of  $b$  the next two levels  $\eta_{3,4}$  approach to each other and at some value  $b_1 > b_0$  become complex conjugated. And so on, so that at large values of  $b$  all low-lying levels are divided on complex conjugated pairs. The corresponding eigenfunctions of these pairs are complex conjugated as well. This fact guarantees the reality of the correlation function.

It is important that all the eigenvalues  $\varepsilon_0$ ,  $\eta_n$  and the eigenfunctions  $\psi_0$ ,  $u_n$  presented in Eq.(20) depend on the parameter  $b$  only. This means that the correlation function and other related physical quantities are universal functions of the scaling parameter  $b$ .

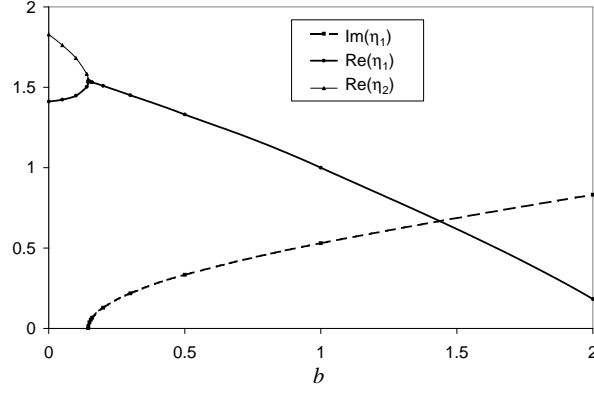


FIG. 2: Dependencies of eigenvalues  $\eta_1$  and  $\eta_2$  on parameter  $b$ . Eigenvalues  $\eta_1$  and  $\eta_2$  are real for  $b < 0.145$ : real part of  $\eta_1$  (thick solid line) and  $\eta_2$  (thin solid line). Eigenvalues  $\eta_1$  and  $\eta_2$  are complex conjugated at  $b > 0.145$ :  $\Re(\eta_1) = \Re(\eta_2)$  (thick solid line) and  $\Im(\eta_1) = -\Im(\eta_2)$  (dashed line).

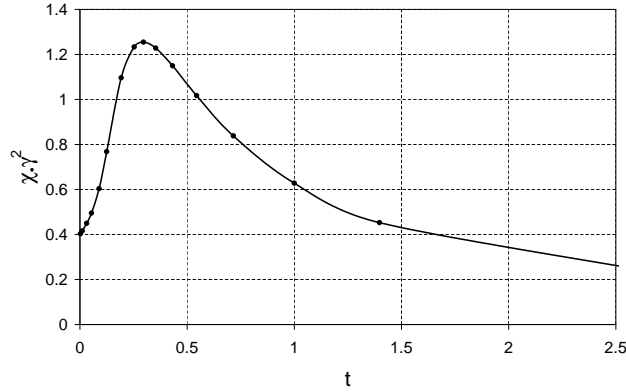


FIG. 3: The dependence of the normalized susceptibility  $\tilde{\chi} = \chi\gamma^2$  on the scaled temperature  $t$ .

In what follows it is convenient to consider the system properties as functions of the scaling parameter  $t = b^{-3/2}$ , which represents the normalized temperature  $t = T/\gamma^{3/2}$ . As shown in the Appendix the excitation energy  $E_{\text{dw}}$  of a chiral domain wall, which separates two domains with different chirality vector, is proportional to  $E_{\text{dw}} \sim \gamma^{3/2}$ . Therefore, the parameter  $t$  is nothing but the ratio (up to numerical factor)  $T/E_{\text{dw}}$  and the physical meaning of the scaling variable  $t$  is the normalization of the temperature by the energy of the chiral domain wall.

According to Eq.(20) the static structure factor is

$$S(k) = \frac{1}{T^{1/3}} \sum_n \langle \psi_0 | u_n \rangle^2 \frac{\eta_n - \varepsilon_0}{(\eta_n - \varepsilon_0)^2 + \tilde{k}^2} \quad (21)$$

where  $\tilde{k} = k/2T^{1/3}$  is the scaled momentum. As follows from Eq.(21), the structure factor is scaled as  $T^{-1/3}$  and, therefore,  $S(k)T^{1/3}$  is the universal function of  $t$ .

The susceptibility  $\chi(k)$  is connected with the static structure factor by the relation  $\chi(k) = S(k)/3T$ . At first, we consider the temperature dependence of the uniform susceptibility  $\chi(0)$ . According to Eq.(21) it is

$$\chi(0) = \frac{1}{3T^{4/3}} \sum_n \frac{\langle \psi_0 | u_n \rangle^2}{\eta_n - \varepsilon_0} \quad (22)$$

Since the eigenfunctions and the eigenvalues of Eqs.(15) and (18) are functions of a single variable  $t$ , the normalized susceptibility  $\tilde{\chi} = \chi\gamma^2$  can be expressed as an universal function of the normalized temperature  $t$ . Thus,  $\tilde{\chi}$  reveals the scaling behavior: in the vicinity of the transition point and at  $T \rightarrow 0$  the dependence of  $\tilde{\chi}$  on the temperature and the model parameter  $\gamma$  enters only in the combination  $T/\gamma^{3/2}$ . The dependence of  $\tilde{\chi}$  on  $t$  is shown in Fig.3. The characteristic features of this dependence are the existence of maximum of  $\tilde{\chi}$  at  $t = t_m$  ( $t_m \simeq 0.432$ ) and the finite value of  $\tilde{\chi}$  at  $T = 0$ . The latter fact is a pure classical effect. In the  $s = 1/2$  quantum F-AF model the ground state is believed to be gapped (though the gap can be extremely small [7]), and so  $\tilde{\chi} \rightarrow 0$  as  $T \rightarrow 0$ . The obtained dependence

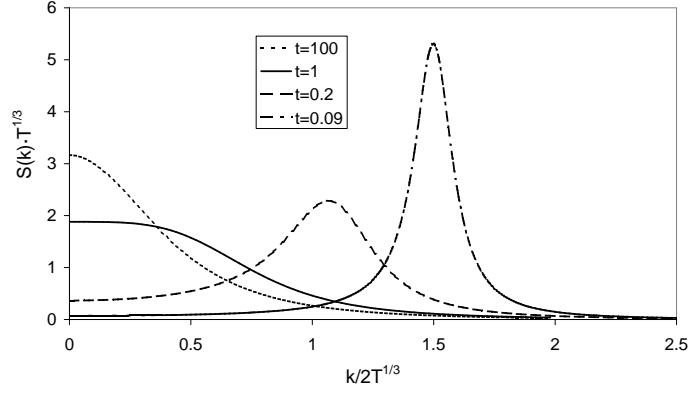


FIG. 4: The static structure factor  $S(k)$  for several values of the scaled temperature  $t$ .

$\tilde{\chi}(t)$  means that for a given model parameter  $\gamma$  the uniform susceptibility has the maximum at temperature  $T_m \sim \gamma^{3/2}$  and the height of this maximum is  $\chi_m \sim \gamma^{-2}$ . This implies that with the increase of  $\gamma$  the maximum of  $\chi$  shifts to higher temperatures and the magnitude of the maximum  $\chi_m$  decreases.

Let us consider the behavior of the static structure factor (21) as a function of  $k$ . Some examples of  $S(k)$  are shown in Fig.4. As we see, the static structure factor has a pronounced maximum and its location depends on  $t$ . In the vicinity of the maximum  $S(k)$  can be represented as

$$S(k) = \frac{S(k_m)}{1 + l_c^2(k - k_m)^2} \quad (23)$$

Therefore, the behavior of the static structure factor is described by three parameters: the location of the maximum  $k_m$ , the magnitude of the maximum  $S(k_m)$ , and the correlation length  $l_c$  characterizing the width of the maximum:

$$l_c^2 = -\frac{1}{2S(k_m)} \frac{d^2 S(k_m)}{dk^2} \quad (24)$$

Obviously, the correlation length is scaled as the space variable (7) and, therefore, the normalized correlation length  $\tilde{l}_c = 2T^{1/3}l_c$  is the universal function of  $t$ .

The location of the maximum  $k_m$  is determined by the condition  $dS/dk = 0$ . According to Eq.(21) this condition reduces to the equation

$$\tilde{k}_m \sum_n \frac{\langle \psi_0 | u_n \rangle^2 (\eta_n - \varepsilon_0)}{[(\eta_n - \varepsilon_0)^2 + \tilde{k}_m^2]^2} = 0 \quad (25)$$

This equation determines the scaled momentum  $\tilde{k}_m$  as a function of  $t$ . Obviously, Eq.(25) always has a trivial solution  $\tilde{k}_m = 0$ . For high values of  $t$  there are no other solutions. However, at some value of the scaled temperature  $t = t_c$  another, non-trivial solution of Eq.(25) with  $\tilde{k}_m \neq 0$  appears. For  $t < t_c$  the maximum of the structure factor shifts from  $\tilde{k}_m = 0$ . Thus,  $t = t_c$  defines the Lifshitz point which corresponds to the transition from the helical to the ferromagnetic phase. Certainly, there is no true helical or ferromagnetic LRO in these phases, because thermal fluctuations destroy any LRO in one-dimensional systems. Therefore, under the helical and the ferromagnetic phases we mean the presence of the short-range order (SRO) of the corresponding type.

The location of the Lifshitz point is determined by the equation:

$$\sum_n \frac{\langle \psi_0 | u_n \rangle^2}{(\eta_n - \varepsilon_0)^3} = 0 \quad (26)$$

The numerical solution of Eq.(26) gives  $t_c \simeq 0.925$ . Thus, the transition line between the ferromagnetic and the helical phases ('Lifshitz boundary') in  $(T, \gamma)$  plane has a form

$$T_c(\gamma) = 0.925\gamma^{3/2} \quad (27)$$

The corresponding phase diagram is shown in Fig.5.

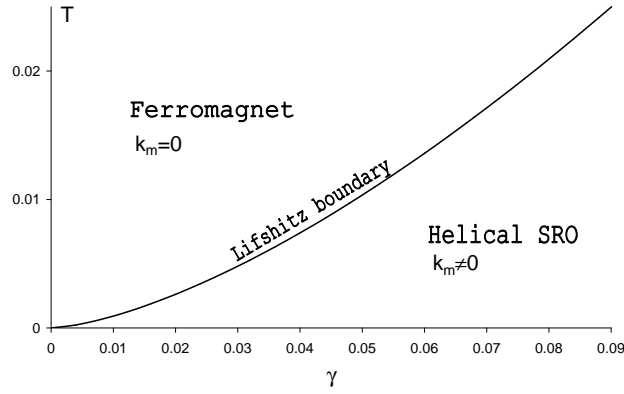
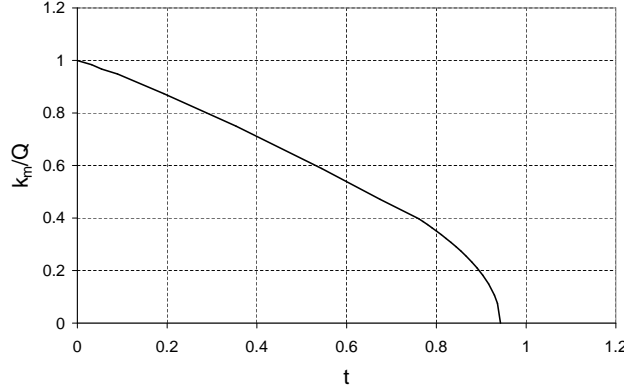
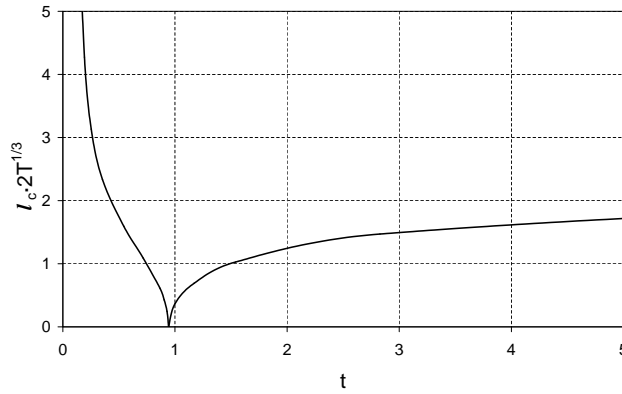


FIG. 5: The phase diagram of model (5).

FIG. 6: The dependence of  $k_m/Q$  ( $Q = \sqrt{2\gamma}$ ) on the scaled temperature  $t$ .

For a fixed model parameter  $\gamma \ll 1$  the dependence of the system properties on the temperature can be qualitatively described in the following way. At  $T = 0$  the structure factor  $S(k)$  has a  $\delta$ -function form at the corresponding wave vectors  $k_m = \pm\sqrt{2\gamma}$ , indicating the helical LRO. At low temperatures ( $T \ll T_c$ ) the  $\delta$ -peaks are smeared by gapless excitations (spin waves) over the helical ground states. The chiral domain wall excitations have the gap ( $E_{dw} \sim \gamma^{3/2}$ ) and their contribution to the thermodynamics is exponentially small. The analysis of Eq.(21) shows that in this region ( $T \ll T_c$ ) the magnitude of the maximum and the correlation length behave as  $S(k_m) \sim l_c \sim \gamma/T$ .

When the temperature is increased, the maximum of  $S(k)$  shifts to  $k = 0$  and at approaching to the Lifshitz point the value of  $k_m$  tends to zero by the square root law  $k_m \sim \gamma^{-1/4}\sqrt{T_c - T}$ . This is similar to the order parameter behavior in Landau theory of second-order phase transitions. Indeed, in the three-dimensional frustrated classical spin model, when the helical LRO exists, the wave vector associated with the helical phase vanishes by the same law

FIG. 7: The dependence of the normalized correlation length  $\tilde{l}_c = 2T^{1/3}l_c$  on the scaled temperature  $t$ .

[20].

The numerically obtained dependencies of  $k_m/\sqrt{2\gamma}$  and the scaled correlation length  $\tilde{l}_c$  on  $t$  are demonstrated in Fig.6 and Fig.7, correspondingly. As shown in Fig.7 the correlation length vanishes at  $t = t_c$ , because  $S(k)$  does not contain  $k^2$  term in  $k$  expansion at the Lifshitz point. The magnitude of the maximum at the Lifshitz point is  $S(0) \approx 1.9\gamma^{-1/2}$ .

For  $T \gg T_c$  the helical correlations are destroyed, the maximum of  $S(k)$  is situated at  $k_m = 0$  and in the limit  $t \rightarrow \infty$  it tends to the results obtained in Ref.[14]:  $S(0) = 3.21/T^{1/3}$  and  $l_c = 1.04/T^{1/3}$ .

Up to now we considered the classical spin model where  $\vec{S}$  is usual three-component classical vector. It is appropriate to discuss briefly the planar model describing by Hamiltonian (2), where the vector  $\vec{S}$  has two components (planar spin model). For short we denote below these two models as  $\nu = 3$  and  $\nu = 2$  cases. Just as for the  $\nu = 3$  model the transition point between the ferromagnetic and the helical ground states for the  $\nu = 2$  model takes place at  $\alpha = 1/4$ . The low-temperature thermodynamics of the  $\nu = 2$  model near the transition point can be analyzed in a similar manner as for the  $\nu = 3$  case. In particular, the calculation of the partition function for the  $\nu = 2$  model reduces to the solution of the Schrödinger equation

$$-\frac{1}{4} \frac{d^2 \psi}{dq^2} + U(q)\psi = \varepsilon \psi \quad (28)$$

where  $U(q) = q^4 - bq^2$ .

Our study of the planar model shows that the thermodynamic quantities are the universal functions of the same scaling parameter  $t = T/\gamma^{3/2}$ . The behaviors of  $S(k)$ ,  $k_m(t)$  and  $l_c(t)$  are similar to that for  $\nu = 3$  case. The Lifshitz point is determined by  $t_c \simeq 0.7$  and the critical exponent characterizing the behavior of  $k_m$  near  $t_c$  is  $1/2$  as well. However, the behavior of the chiral correlation function

$$R_l = \langle \vec{K}_n \cdot \vec{K}_{n+l} \rangle \quad (29)$$

of these two models are different. In the continuum approach the chiral vector is expressed as

$$\vec{K}_n = \vec{S}_n \times \vec{S}_{n+1} \approx \vec{s}(x) \times \frac{\partial \vec{s}(x)}{\partial x} \quad (30)$$

In the  $\nu = 2$  model the chiral vector is directed perpendicular to the spin plane for any  $x$ . Therefore in this case

$$\vec{K}(l) \cdot \vec{K}(0) \approx \frac{\partial \vec{s}(l)}{\partial x} \cdot \frac{\partial \vec{s}(0)}{\partial x} = q(l)q(0) \quad (31)$$

In the  $\nu = 3$  model we take into account local coordinates with  $\vec{s} = (0, 0, 1)$  and  $q_z = 0$  and obtain similar expression

$$\vec{K}(l) \cdot \vec{K}(0) = \mathbf{q}(l) \cdot \mathbf{q}(0) \quad (32)$$

The expression for the chiral correlation function  $R_l$  can be obtained in the same manner as for the spin correlation function:

$$R_l = \sum_n \langle \psi_0 | \mathbf{q} | \psi_n \rangle^2 e^{-2T^{1/3}(\varepsilon_n - \varepsilon_0)l} \quad (33)$$

Here  $\psi_n$  and  $\varepsilon_n$  are the eigenfunctions and the eigenvalues of the Schrödinger equations (15). For planar case  $R_l$  has similar expression where  $\psi_n$  and  $\varepsilon_n$  are solutions of Eq.(28). Since  $\psi_n$  and  $\varepsilon_n$  are always real, the chiral correlation function  $R_l$  does not oscillate and the maximum of the corresponding structure factor is at  $k = 0$  for both  $\nu = 2$  and  $\nu = 3$  cases.

As follows from Eq.(33) the correlation length of the chirality  $\zeta$  is scaled as  $T^{1/3}$  and at  $T \rightarrow 0$  it is defined by the lowest level having the non-zero matrix element with the ground-state wave function  $\psi_0$ . So, for normalized chiral correlation length  $\tilde{\zeta} = 2T^{1/3}\zeta$  we have

$$\tilde{\zeta} = \frac{1}{\varepsilon_1 - \varepsilon_0} \quad (34)$$

The ground state wave function for Eq.(28) is an even function of  $q$  and only the eigenfunctions with odd parity give contributions to  $R_l$ . So, for the  $\nu = 2$  model  $\varepsilon_1$  is the energy of the first excited state of the odd parity. For the  $\nu = 3$  model the matrix elements in Eq.(33) are non-zero only for the wave functions  $\psi_n$  with  $l_z = 1$ . At the transition



point (corresponding to the limit  $t \rightarrow \infty$ ) the energy difference  $\varepsilon_1 - \varepsilon_0$  is finite for both  $\nu = 2$  ( $\varepsilon_1 - \varepsilon_0 = 1.09$ ) and  $\nu = 3$  ( $\varepsilon_1 - \varepsilon_0 = 1.21$ ) cases.

At  $t \rightarrow 0$  the behavior of the energy gap between two lowest levels for  $\nu = 2$  and  $\nu = 3$  models becomes qualitatively different. For the  $\nu = 2$  case the potential  $U(q) = q^4 - bq^2$  has two degenerate minima and the splitting of two lowest levels  $\varepsilon_1 - \varepsilon_0$  depends upon tunneling through the classically forbidden region of small  $q$ . This tunneling is exponentially small for low temperatures and the WKB estimate gives  $\tilde{\zeta} \sim \exp(1/3\sqrt{2}t)$ . However, for the  $\nu = 3$  case the particle moves in two-dimensional axially symmetric potential, the form of the Mexican hat, and relevant splitting is equal to the additional energy associated with one unit of the angular momentum. Then, according to Eq.(16)  $\tilde{\zeta} = 4/t^{2/3}$ . Thus, the behavior of the correlation length of the chirality is essentially different for these two models.

So far we studied the helical side of the transition point  $\alpha > 1/4$  ( $\gamma > 0$ ). On the ferromagnetic side ( $\gamma < 0$ ) the static structure factor  $S(k)$  and the susceptibility  $\chi(k)$  have the maximum at  $k = 0$  for any temperature. The uniform susceptibility  $\chi$  diverges at  $T \rightarrow 0$  but the corresponding exponent changes from  $4/3$  to  $2$  and Eq.(22) describes this crossover. The exponent  $2$  appears in the limit  $b \rightarrow -\infty$ , when  $\tilde{\chi}(b) = -2b^3/3$  and the susceptibility becomes  $\chi = 2|\gamma|/3T^2$ , which is in accord with the result for HF with the coupling constant  $|\gamma|$ . Indeed, in the limit  $b \rightarrow -\infty$  one can neglect the second derivative term in energy functional (5) and the model reduces to the HF with renormalized coupling  $|\gamma|$ .

#### IV. SUMMARY

We have studied the low-temperature thermodynamics of the classical F-AF model in the vicinity of the ferromagnet-helimagnet transition point with use of the continuum approximation. The calculation of the partition and the spin correlation functions is reduced to a quantum mechanical problem of a particle in a potential well. It is shown that the thermodynamic quantities are universal functions of the scaling variable  $t = T/\gamma^{3/2}$ , where  $\gamma = 4J_2/|J_1| - 1$  describes the deviation from the transition point.

On the ferromagnetic side ( $\gamma < 0$ ) the static structure factor  $S(k)$  has the maximum at  $k = 0$  for all temperatures. The uniform susceptibility  $\chi$  diverges at  $T \rightarrow 0$  but the corresponding asymptotics changes from  $\chi \sim T^{-4/3}$  at the transition point to  $\chi \sim |\gamma|/T^2$  for  $T \ll |\gamma|^{3/2}$ . The crossover between these regimes takes place at  $T \sim \gamma^{3/2}$ .

On the helical side of the transition point ( $0 < \gamma \ll 1$ ) our investigation displays the following dependence of the system properties on the temperature. At zero temperature the static structure factor  $S(k)$  has a  $\delta$ -function form at the corresponding wave vectors  $k_m = \pm\sqrt{2\gamma}$ , indicating the LRO of the helical-type. At finite temperatures the LRO is destroyed by thermal fluctuations, which is manifested in smearing of  $\delta$ -peaks of the static structure factor by gapless excitations (spin waves) over the helical ground states. The chiral domain wall excitations have the gap ( $E_{dw} \sim \gamma^{3/2}$ ) and their contribution to the thermodynamics is exponentially small for low temperatures  $T \ll \gamma^{3/2}$ . In this region the magnitude of the maximum of the structure factor and the correlation length behave as  $S(k_m) \sim l_c \sim \gamma/T$ .

Further increase of the temperature is accompanied by the damping of the peak and its shift to  $k = 0$ . At approaching to the Lifshitz point  $T \rightarrow T_c = 0.925\gamma^{3/2}$  the value of  $k_m$  tends to zero by the square root law  $k_m \sim \gamma^{-1/4}\sqrt{T_c - T}$ . Such dependence is similar to the order parameter behavior in the Landau theory of the second-order phase transitions. So, the location of the peak  $k_m$  plays a role of the order parameter, though one should remember that the system has only the short-range helical order at finite temperatures. Equation  $T_c = 0.925\gamma^{3/2}$  determines the Lifshitz boundary in  $(T, \gamma)$  plane, separating the ferromagnetic and the helical phases.

For  $T > T_c$  the helical correlations are destroyed by the chiral domain wall excitations and the maximum of the static structure factor  $S(k)$  is situated at  $k_m = 0$ . The high temperature limit  $T \gg T_c$  is equivalent to the limit  $\gamma \ll T^{2/3}$ . This implies that one can neglect the second terms in Eqs.(2) and (5) and the model effectively reduces to that at the transition point studied in Ref.[14]. Here the uniform susceptibility and the correlation length are  $\chi(0) = 1.07/T^{4/3}$  and  $l_c = 1.04/T^{1/3}$ . We should remind that our analysis is restricted by low temperatures and, therefore, the latter high- $T$  limit is in fact restricted by  $T_c \ll T \ll 1$ .

The uniform susceptibility  $\chi$  has the maximum at  $T_m \sim \gamma^{3/2}$  and  $\chi_m \sim \gamma^{-2}$ , i.e. with the increase of the frustration parameter  $\alpha$  the maximum of  $\chi$  shifts to higher temperatures and the magnitude of the maximum  $\chi_m$  decreases. The obtained dependence of  $\chi$  on  $T$  is in a qualitative agreement with those observed in the edge-shared compounds with  $\alpha$  close to  $1/4$  (*Li<sub>2</sub>CuO<sub>2</sub>* [2], *Rb<sub>2</sub>Cu<sub>2</sub>Mo<sub>3</sub>O<sub>12</sub>* [3], *Li<sub>2</sub>CuZrO<sub>4</sub>* [13]). The dependencies of  $T_m$  and  $\chi_m$  on the frustration parameter  $\alpha$  are also in accord with the experimental observations [13].

We have also shown that the thermodynamic behavior of both planar and classical F-AF models are similar. The exception is the chiral correlation function. The chiral correlation length of the planar model increases exponentially at  $T \rightarrow 0$  in contrast with the power dependence for the classical  $\nu = 3$  model. This fact is explained by different topology of the potentials in the corresponding Schrödinger equations.

It is interesting to compare our results with those obtained in Refs.[16, 17] for intermediate values of  $T$  and  $\gamma$ . In contrast with the phase diagram obtained for small values of  $T$  and  $\gamma$  and schematically shown in Fig.6, the Lifshitz

boundary for intermediate values of  $T$  and  $\gamma$  can have the reentrant behavior [16]. There is a critical value of  $\gamma = \gamma_c$  (for the planar model  $\gamma_c \simeq 0.16$  [16]), where the Lifshitz boundary turns round and moves back to  $\gamma = 0$  with the further increase of temperature. This means that for a fixed small value of  $\gamma$  ( $0 < \gamma < \gamma_c$ ) the ferromagnetic phase exists in the finite range of temperatures and for  $\gamma > \gamma_c$  the helical-type correlations remain for all temperatures. This fact testifies that in the region of intermediate or large values of  $T$  and  $\gamma$ , where the continuum approximation becomes unapplicable, the thermodynamic behavior can be qualitatively different from the results presented here for small  $T$  and  $\gamma$ .

## Appendix

In the appendix we calculate the chiral domain wall energy for the classical spin model described by energy functional (5). To study excitations in this model it is useful to make the following rescaling of the space variable  $x = \xi/\sqrt{2\gamma}$ . Then, energy functional (5) takes the form:

$$E = \frac{\gamma^{3/2}}{2^{3/2}} \int d\xi \left[ \left( \frac{\partial^2 \vec{s}}{\partial \xi^2} \right)^2 - 2 \left( \frac{\partial \vec{s}}{\partial \xi} \right)^2 \right] \quad (\text{A.1})$$

Here we see that the integrand in Eq.(A.1) does not contain any parameter and, therefore, any localized excitation is proportional to  $\sim \gamma^{3/2}$ . Certainly, the determination of the numerical factor before  $\gamma^{3/2}$  needs the solution of the corresponding Euler equation. These Euler equations are highly non-linear and its complete analysis is hardly possible. Fortunately, such an analysis is possible for the planar spin case. The solutions for the planar spin case represent particular cases of solutions for the original three-component spin model.

For the planar model the two-component spin vector can be represented as  $\vec{s} = (\sin \theta, \cos \theta)$  and energy functional (A.1) in terms of  $\theta(x)$  has a form

$$E = \frac{\gamma^{3/2}}{2^{3/2}} \int d\xi \left[ \left( \frac{\partial^2 \theta}{\partial \xi^2} \right)^2 + \left( \frac{\partial \theta}{\partial \xi} \right)^4 - 2 \left( \frac{\partial \theta}{\partial \xi} \right)^2 \right] \quad (\text{A.2})$$

Variation of energy functional (A.2) in  $\theta(\xi)$  leads to the Euler equation

$$\frac{\partial^4 \theta}{\partial \xi^4} - 6 \frac{\partial^2 \theta}{\partial \xi^2} \left( \frac{\partial \theta}{\partial \xi} \right)^2 + 2 \frac{\partial^2 \theta}{\partial \xi^2} = 0 \quad (\text{A.3})$$

Here we see that the Euler equation has a trivial helical solution  $\theta(\xi) = a(\xi - \xi_0)$  with any constants  $a$  and  $\xi_0$ . However, the minimum of energy (A.2) corresponding to the ground state is achieved by a definite helical configuration with

$$\theta(\xi) = \pm(\xi - \xi_0) \quad (\text{A.4})$$

and the ground state energy is

$$E_0 = -L \frac{\gamma^2}{2} \quad (\text{A.5})$$

To find the excitations over the helical ground state we should look for other solutions of Eq.(A.3). Eq.(A.3) can be integrated so that for  $y(\xi) = \partial \theta / \partial \xi$  we obtain equation

$$y'^2 = y^4 - 2y^2 + Ay + B \quad (\text{A.6})$$

with some integration constants  $A$  and  $B$ .

The energy functional in terms of  $y(\xi)$  takes the form:

$$E - E_0 = \frac{\gamma^{3/2}}{2^{3/2}} \int d\xi [y'^2 + (1 - y^2)^2] \quad (\text{A.7})$$

The right-hand side of Eq.(A.6) has a double-well form. The complete analysis of solutions of Eq.(A.6) will be given elsewhere. Here we present the solution describing the chiral domain wall only. This case corresponds to the choice of integration constants  $A = 0$  and  $B = 1$ . In this case the solution of Eq.(A.6) has a simple form

$$y(\xi) = \tanh(\xi - \xi_0) \quad (\text{A.8})$$

or in original terms for angle  $\theta(x)$

$$\theta(x) = \theta_0 + \ln \left[ \cosh \left( \sqrt{2\gamma}(x - x_0) \right) \right] \quad (\text{A.9})$$

with arbitrary  $\theta_0$  and  $x_0$ . As can be seen, this solution describes a chiral domain wall separating two domains of opposite chirality. The energy of this excitation is

$$E_{\text{dw}} = \frac{1}{3}(2\gamma)^{3/2} \quad (\text{A.10})$$

In case of three-component spin vectors the chiral domain wall excitations are more complicated. They depend on the boundary conditions on  $x = \pm\infty$ , which can be imposed on the chiral vectors  $\vec{K}$ . In the helical ground state the length of the chiral vectors equals  $|\vec{K}| = \sqrt{2\gamma}$ , but the direction is arbitrary according to degeneracy of the helical ground state. Therefore, the chiral domain wall solution is a function of the angle between the chiral vectors at  $x = \pm\infty$ :

$$\cos \phi = \frac{(\vec{K}_{-\infty} \cdot \vec{K}_{\infty})}{2\gamma} \quad (\text{A.11})$$

In the planar spin case considered above the angle  $\phi$  is  $\phi = \pi$ , because chiral vectors are antiparallel on  $\pm\infty$ . It is also obvious that the limit  $\phi \rightarrow 0$  corresponds to the ground state configuration. In general the dependence of the energy of the chiral domain wall on the angle  $\phi$  is unknown, but it is natural to assume that this function monotonically increases from zero at  $\phi = 0$  to the exact result Eq.(A.10) at  $\phi = \pi$ . Therefore, in any case the energy of the chiral domain wall is proportional to  $\sim \gamma^{3/2}$  and can be written as

$$E_{\text{dw}} = f(\phi)\gamma^{3/2} \quad (\text{A.12})$$

with some smooth monotonic function  $f(\phi)$  having the limits  $f(0) = 0$  and  $f(\pi) = 2^{3/2}/3$ .

- 
- [1] H.-J. Mikeska and A. K. Kolezhuk, in *Quantum Magnetism*, Lecture Notes in Physics Vol. **645**, edited by U. Schollwöck, J. Richter, D. J. J. Farnell, and R. F. Bishop, Eds. (Springer-Verlag, Berlin, 2004), p. 1.
  - [2] Y. Mizuno, T. Tohyama, S. Maekawa, T. Osafune, N. Motoyama, H. Eisaki, and S. Uchida, Phys. Rev. B **57**, 5326 (1998).
  - [3] M. Hase, H. Kuroe, K. Ozawa, O. Suzuki, H. Kitazawa, G. Kido and T. Sekine, Phys. Rev. B **70**, 104426 (2004).
  - [4] S.-L. Drechsler, J. Malek, J. Richter, A. S. Moskvina, A. A. Gippius, and H. Rosner, Phys. Rev. Lett. **94**, 039705 (2005).
  - [5] J. Malek, S.-L. Drechsler, U. Nitzsche, H. Rosner, and H. Eschrig, Phys. Rev. B **78**, 060508(R) (2008).
  - [6] A. V. Chubukov, Phys. Rev. B **44**, 4693 (1991).
  - [7] C. Itoi and S. Qin, Phys. Rev. B **63**, 224423 (2001).
  - [8] D. V. Dmitriev and V. Ya. Krivnov, Phys. Rev. B **73**, 024402 (2006).
  - [9] F. Heidrich-Meisner, A. Honecker, and T. Vekua, Phys. Rev. B **74**, 020403(R) (2006).
  - [10] H. T. Lu, Y. J. Wang, S. Qin, and T. Xiang, Phys. Rev. B **74**, 134425 (2006).
  - [11] D. V. Dmitriev, V. Ya. Krivnov, and J. Richter, Phys. Rev. B **75**, 014424 (2007).
  - [12] T. Hikihara, L. Kecke, T. Momoi, and A. Furusaki, Phys. Rev. B **78**, 144404 (2008).
  - [13] S.-L. Drechsler, O. Volkova, A. N. Vasiliev, N. Tristan, J. Richter, M. Schmitt, H. Rosner, J. Malek, R. Klingeler, A. A. Zvyagin, B. Buchner, Phys. Rev. Lett. **98**, 077202 (2007).
  - [14] D. V. Dmitriev and V. Ya. Krivnov, Phys. Rev. B **82**, 054407 (2010).
  - [15] M. E. Fisher, Am. J. Phys. **32**, 343 (1964).
  - [16] I. Harada, J. Phys. Soc. Jpn. **53**, 1643 (1984).
  - [17] I. Harada and H. J. Mikeska, Z. Phys. B **72**, 391 (1988).
  - [18] R. Pandit and C. Tannous, Phys. Rev. B **28**, 281 (1983); T. Delica, R. W. Gerling and H. Leschke, Physica Scripta **35**, 57 (1987).
  - [19] D. V. Dmitriev and V. Ya. Krivnov, Phys. Rev. B **81**, 054408 (2010).
  - [20] S. Redner and H. E. Stanley, Phys. Rev. B **16**, 4901 (1977).